



## Power Supply Design Seminar

# LLC Converter Small Signal Modeling

Reproduced from  
2014 Texas Instruments Power Supply Design Seminar  
SEM2100,  
Topic 7  
TI Literature Number: SLUP329

© 2014, 2015 Texas Instruments Incorporated

Power Seminar topics and online power-  
training modules are available at:  
[ti.com/psds](http://ti.com/psds)

# LLC Converter Small Signal Modeling

Brent McDonald

## ABSTRACT

*Control loop modeling of power supplies is essential for efficient optimization of the power supply stability requirements as well as meeting key line and load transient performance requirements. While this is obvious to the power supply designer, it is equally obvious that a practical small signal model for the LLC converter is glaringly missing from the designer's tool box. This is compounded by the rise of demanding efficiency requirements. In some cases the total efficiency of the power supply must be 96%, while maintaining a high power factor and low total harmonic distortion. Requirements like this are putting significant pressure on the DC-DC stage to deliver efficiency in excess of 96%. Resonant LLC converters are a natural choice due to their ability to achieve these high efficiencies. Unfortunately, the absence of a user friendly small signal model has made the topology significantly more difficult to work with.*

80 PLUS Certification	115-V Internal Non-redundant				230-V Internal Redundant			
% of Rated Load	10%	20%	50%	100%	10%	20%	50%	100%
80 PLUS	–	80%	80%	80%	N/A			
80 PLUS Bronze	–	82%	85%	82%	–	81%	85%	81%
80 PLUS Silver	–	85%	88%	85%	–	85%	89%	85%
80 PLUS Gold	–	87%	90%	87%	–	88%	92%	88%
80 PLUS Platinum	–	90%	92%	89%	–	90%	94%	91%
80 PLUS Titanium	–	–	–	–	90%	94%	96%	91%

Courtesy: <http://www.plugloadsolutions.com/80PlusPowerSupplies.aspx>

Table 1 – 80 PLUS certification requirements.

*This topic provides the power supply designer with a small signal model for the LLC converter and a practical set of tools that enables the application of the model to a wide range of operating conditions. In addition, the modeling tools provide the designer with an extensive set of time domain and spectral analysis outputs that are extremely useful in understanding the end performance characteristics of their design. This model and the associated tools represent a huge addition to the power supply designer's tool box, enabling significant design aid and control loop insight to the LLC converter.*

## I. INTRODUCTION – THE LLC CONVERTER

Historically, buck-derived topologies have dominated the design choices in DC-DC converters. These topologies include the buck, push-pull, forward, half-bridge, full-bridge, phase-shifted full-bridge, etc. While it seems that there is an endless myriad of variations of this theme, all of these circuits fundamentally behave as a buck converter. In this context, they all offer an intuitive venue for the designer to both understand and subsequently derive the appropriate compensation for control. In each case the fundamental operation of the converter can be understood as a combination

of switches that generate a high constant-frequency square-wave with a variable duty cycle. This square-wave is processed by a low pass filter to generate a DC output voltage. Since the low pass filter is usually composed of an inductor and a capacitor, classic small signal modeling techniques are employed to generate the model for the resulting second-order plant. Control of the output voltage is easily achieved by varying the duty cycle of the square-wave. This kind of intuition and modelling of a buck-converter is not extendable to the LLC converter.

Figure 1 shows a classic  $\frac{1}{2}$  bridge LLC converter. This converter operates by creating a constant duty cycle, variable frequency square

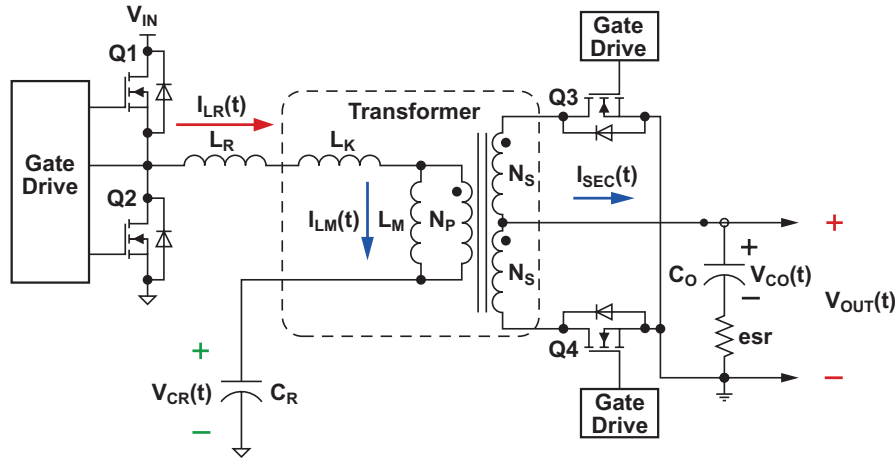


Figure 1 – LLC ½ bridge converter.

wave at the drain of Q2. A band-pass filter composed of  $L_R$ ,  $L_K$ ,  $L_M$  and  $C_R$  filters the square wave. The filter removes both the high and low frequency components of the input signal, leaving the dominate resonant frequency circulating in the tank. Conceptually this waveform is a current that is rectified by Q3 and Q4 and dumped into the output capacitor  $C_O$  to create the DC output voltage  $V_{OUT}(t)$ . Modulating the frequency of the input square wave at the drain of Q2 controls the output. Changes in the operating frequency change the impedance of the tank network, allowing the tank current to increase at lower frequencies or decrease with higher frequencies. The frequency dependent nature of the tank enables frequency modulation to regulate the output voltage.

State Variable
$I_{LR}(t)$
$I_{LM}(t)$
$V_{CR}(t)$
$V_{CO}(t)$

Table 2 – State variables.

As an example, the output voltage is derived from these values through the following equation. The state-variables are highlighted in **bold**. All other variables are either system inputs or constants.

$$V_{OUT}(t) = V_{CO}(t) + \left( \mathbf{I_{LR}(t)} - \mathbf{I_{LM}(t)} \right) \frac{N_P}{N_S} - I_{OUT}(t) \text{ esr}$$

The next concept that is critical to this discussion is that of converter-states. Simply put, a converter-state is a given set of conditions where the MOSFETs of Figure 1 are either on or off. Since there are 4-MOSFETs in Figure 1 there are a total of 16 possible states. In order to simplify this discussion, several states are eliminated. For example, all states related to Q1 and Q2 being on at the same time (or Q3 and Q4) will be ignored since they have no practical value to the converter and only result in damage to the power supply. In addition, the state where Q1 and Q2 are both off is also ignored. Although this is a perfectly valid operating state, the discussion is easier to follow if this is ignored, and as will be shown later, it is not necessary in order to achieve reasonably accurate results. Table 3 shows a comprehensive list of the different states that are discussed in this paper.

State	Q1	Q2	Q3	Q4
1	ON	OFF	OFF	ON
2	ON	OFF	ON	OFF
3	ON	OFF	OFF	OFF
4	OFF	ON	OFF	ON
5	OFF	ON	ON	OFF
6	OFF	ON	OFF	OFF

Table 3 – Converter states.

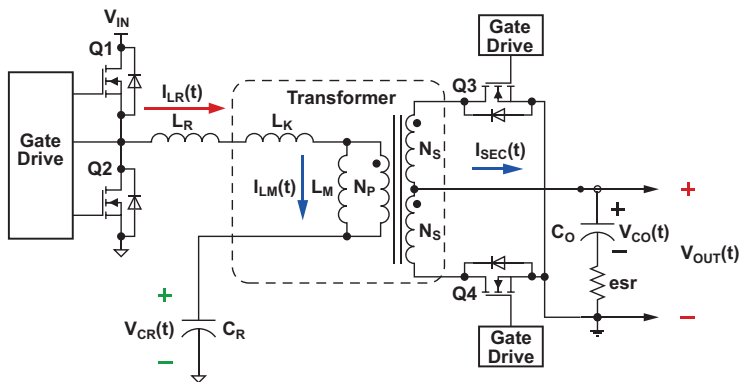
A sequence of the states from Table 3 creates an operating mode. There are many different possible operating modes constructed from this table; however, there are three that are the most common in practice. They are: resonance, below-resonance and above resonance.

Figure 2 shows the first mode – resonance. In this mode Q1 and Q2 are turned on and off at a frequency equal to the resonant frequency of the system:

$$\frac{1}{2\pi\sqrt{(L_R + L_K)C_R}}$$

In this same figure the input voltage is adjusted so that when Q1 and Q2 are modulated in this way

the DC output voltage is exactly equal to  $\frac{1}{2}$  the input voltage. Q3 and Q4 have no dead time and therefore also operate at exactly 50% duty cycle. The net result is there are only 2 states used: 1 and 5. The operation of those states is highlighted in the table shown in Figure 2 as well as on the waveforms. Therefore, regulation is achieved by oscillating back and forth from state 1 to state 5.



### Mode State Sequence: 1→5

State	Q1	Q2	Q3	Q4
1	ON	OFF	OFF	ON
2	ON	OFF	ON	OFF
3	ON	OFF	OFF	OFF
4	OFF	ON	OFF	ON
5	OFF	ON	ON	OFF
6	OFF	ON	OFF	OFF

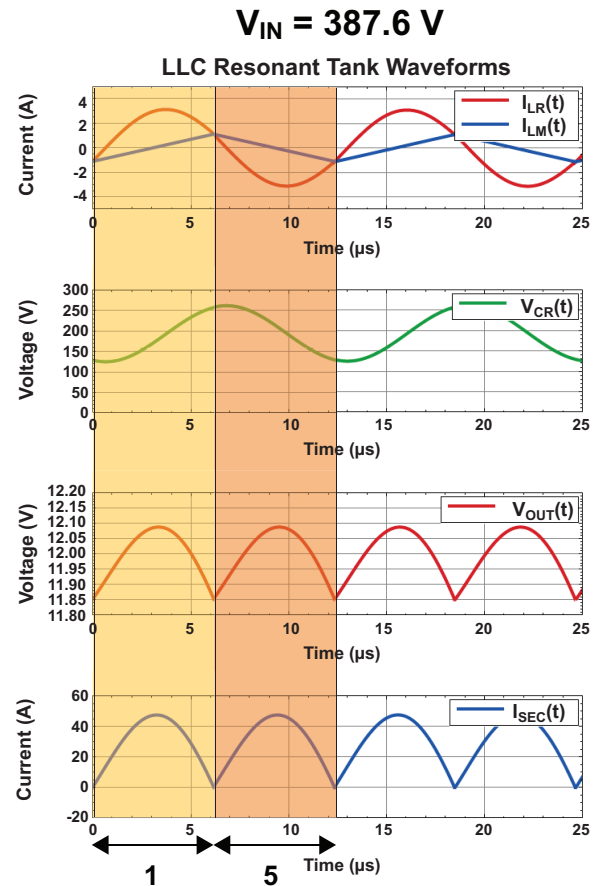
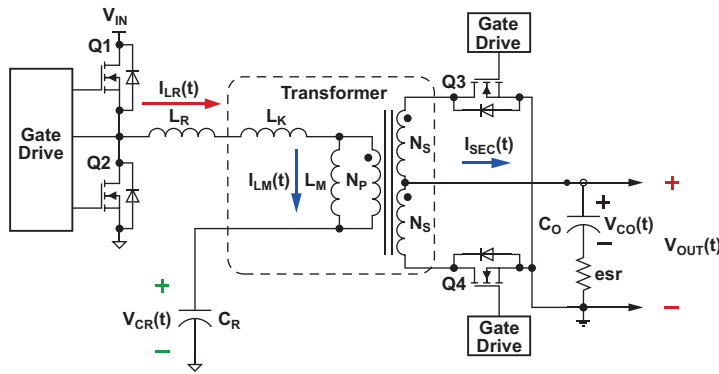


Figure 2 – Mode – resonance.

The next mode discussed is below-resonance. This is illustrated in Figure 3. In this case the mode state sequence is 1→3→5→6. Conceptually the operation is similar to that of the resonant-mode. States 1 and 5 are identical to those used in the previous mode and represent the energy transfer mechanism. The difference is states 3 and 6 are interleaved into the mode. These additional states appear in the mode when  $I_{LR}(t)=I_{LM}(t)$ . When this happens the voltage on the resonant capacitor

$V_{CR}(t)$  becomes large enough to reverse bias the diodes on the secondary. Although Q3 and Q4 are MOSFETs, it is important to remember that they operate as ideal diodes and therefore shut off when their  $V_{DS}$  is less than 0 V. Once they shut off, current continues to flow through  $I_{LR}(t)$ . This current subsequently results in a larger voltage movement on  $V_{CR}(t)$ . The increased peak-to-peak voltage on  $V_{CR}(t)$  is what forces the current  $I_{LR}(t)$  to go to a larger peak value.



### Mode State Sequence: 1→3→5→6

State	Q1	Q2	Q3	Q4
1	ON	OFF	OFF	ON
2	ON	OFF	ON	OFF
3	ON	OFF	OFF	OFF
4	OFF	ON	OFF	ON
5	OFF	ON	ON	OFF
6	OFF	ON	OFF	OFF

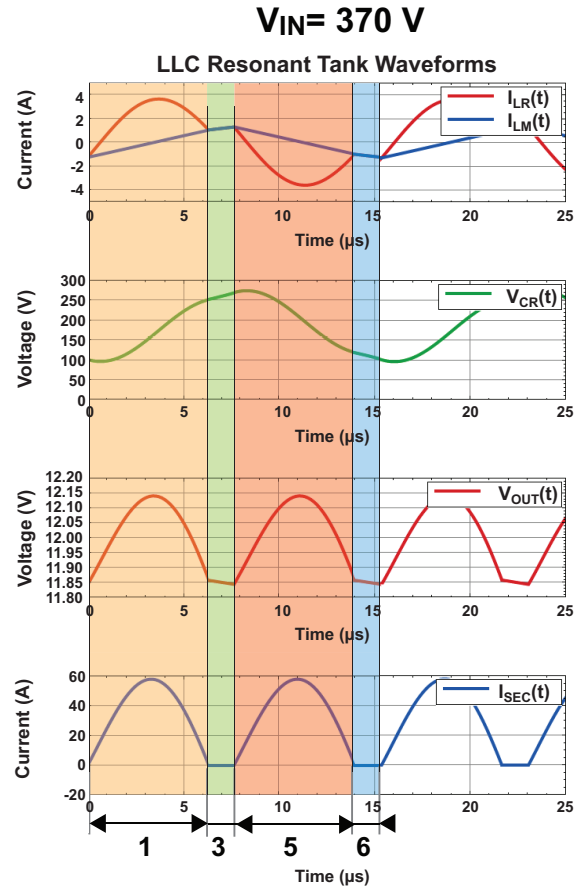


Figure 3 – Mode – Below resonance.

The next mode discussed is above-resonance, illustrated in Figure 4. In this case the mode state sequence is 1→4→5→2. Like the previous two modes, states 1 and 5 are used as the primary energy transfer mechanism; however, in this mode, states 4 and 2 are also utilized. These two new states now allow energy to transfer to the load

through the opposite synchronous rectifier. This is illustrated in the waveform plot in Figure 4 by the narrow shaded regions labeled as 4 and 2. As will be seen later, this difference in the energy transfer mechanism can have dramatic results on the overall small-signal response.

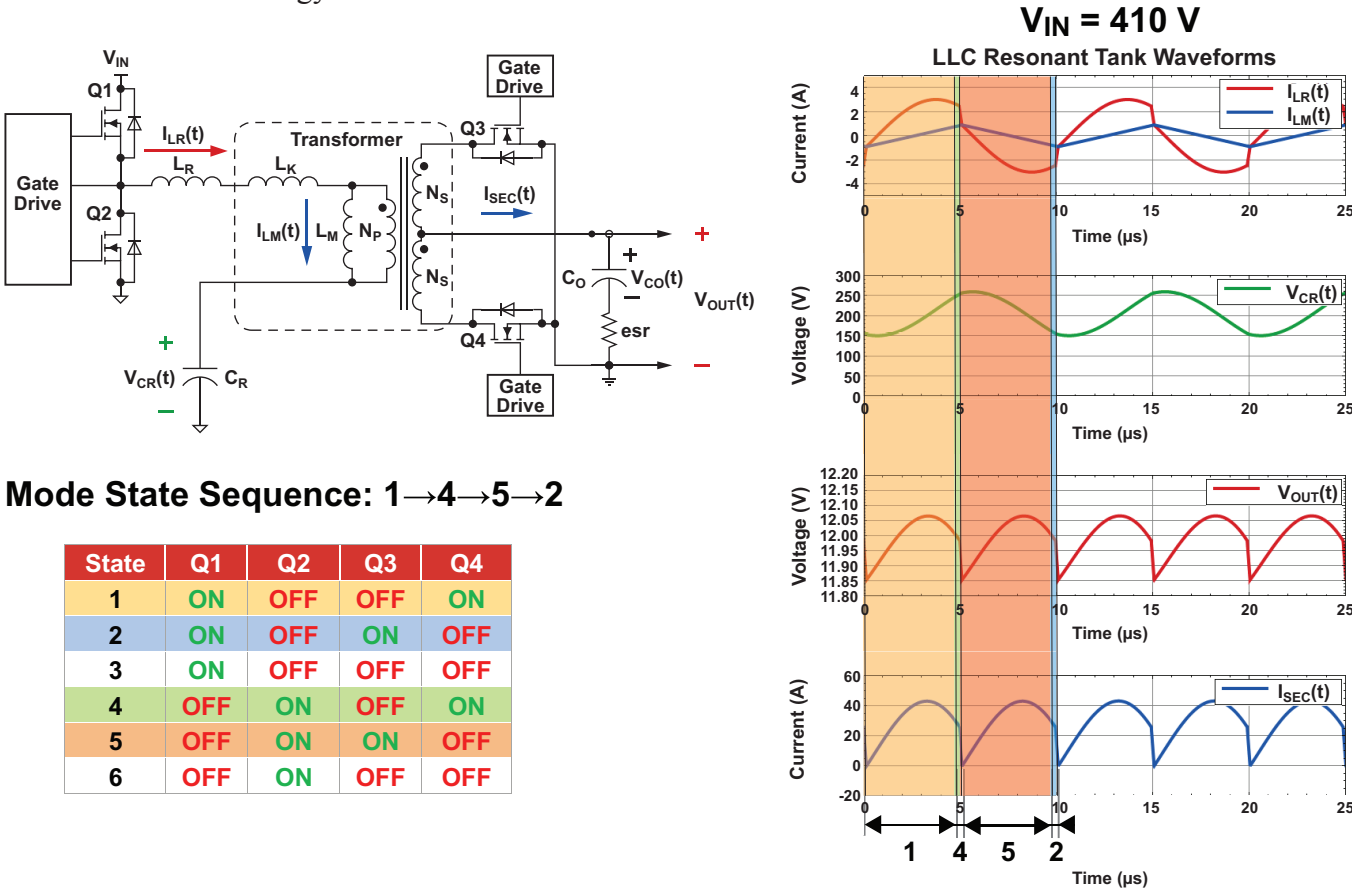


Figure 4 – Mode – Above resonance.

## II. THE SMALL SIGNAL MODELLING PROCESS

Now that all the necessary ground work has been laid, the next step is to take the state-variables along with the mode and the relevant operating states and come up with a way to model the small-signal dynamics. Figure 5 illustrates the modelling process. Essentially, an LLC converter is a non-linear, time-varying system. That is just a complicated way of saying that it is not possible to use traditional small signal modeling tools like the Bode plot. In order to do this the behavior of the actual system is approximated with a system that is linear and time-invariant. This, in essence, is the goal of the modelling process as illustrated in Figure 5.

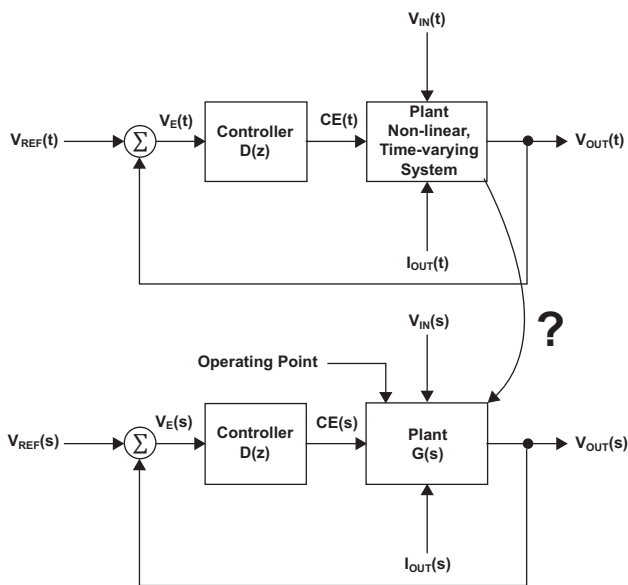


Figure 5 – The small signal modeling process.

In order to derive a system that is linear, time-invariant and reasonably accurate the following three steps must be completed:

- (1) Calculate the steady-state operating point
- (2) Average the differential equations of the state-variables across the different states used in each operating mode
- (3) Linearize the result of step (2) at the operating point determined in step (1)

In power supplies, either the so-called state-space-averaging method or circuit averaging method, historically, best illustrates the averaging process.

### A. Averaging

#### i. State Space Averaging

In order to understand the state-space-averaging process, consider the simple constant frequency, variable duty cycle buck converter shown in Figure 6. In this same figure, 3 distinct operating states are explicitly drawn. For a system operating in continuous conduction mode (CCM) only states 2 and 3 are used. The key system waveforms are shown in Figure 7. Color is used to highlight which state is operable at any given time.

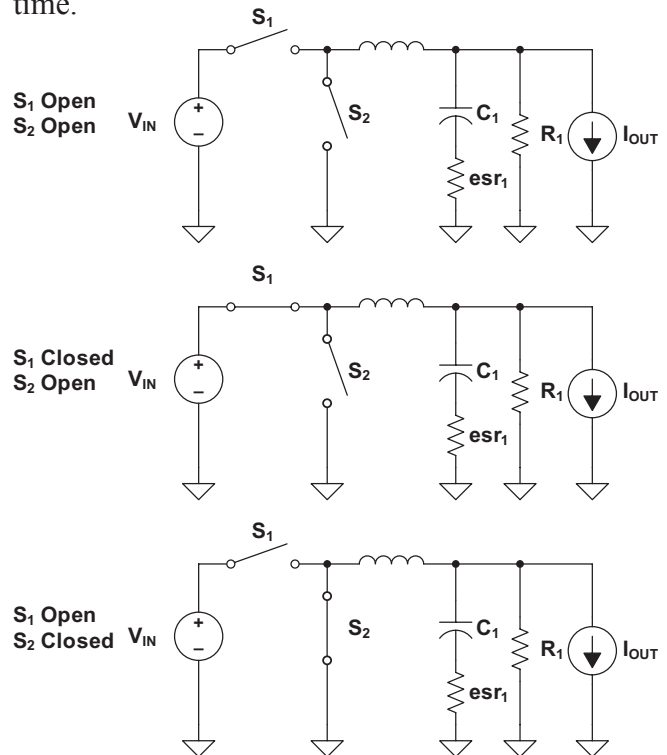


Figure 6: Buck converter.



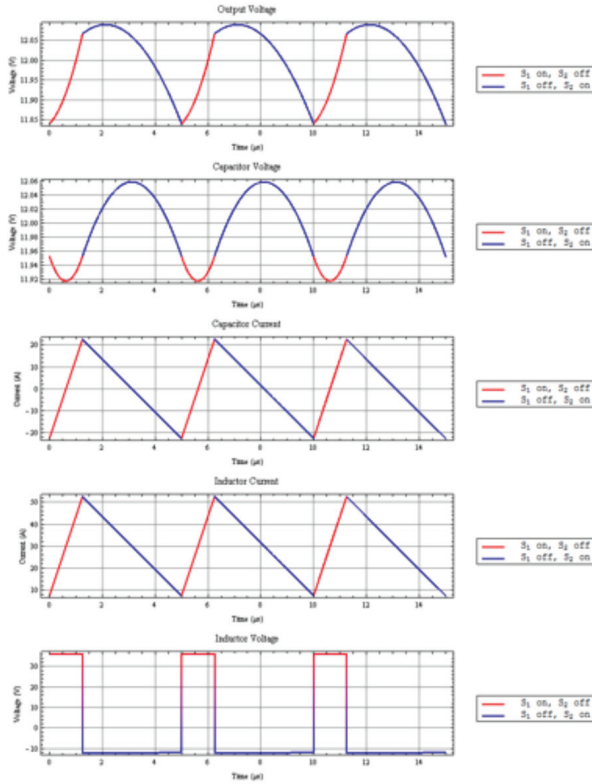


Figure 7: Buck waveforms.

State space averaging works by recognizing that each state of the system can be modeled by a differential equation. Generalized forms of these differential equations are shown here:

$$\text{State 1: } \dot{x}(t) = A_1 \cdot x(t) + B_1 \cdot u(t)$$

$$\text{State 2: } \dot{x}(t) = A_2 \cdot x(t) + B_2 \cdot u(t)$$

State 1 only applies to the system for a portion of the operating period. This portion is denoted by  $d(t)$  in the equations below in Table 4. Likewise state 2 applies for the remainder of the period  $(1-d(t))$ . Applying these percentages to the equations and adding the results together produces an averaged result.

Description	Equation
Averaged system	$\dot{\tilde{x}}(t) = A \cdot \tilde{x}(t) + B \cdot u(t)$
Average value of the state matrix A	$A = A_1 \cdot d(t) + A_2 \cdot (1 - d(t))$
Average value of the matrix B	$B = B_1 \cdot d(t) + B_2 \cdot (1 - d(t))$
Overall averaged system	$\dot{\tilde{x}}(t) = d(t) \cdot x(t) \cdot (A_1 - A_2) + d(t) \cdot u(t) \cdot (B_1 - B_2) + A_2 \cdot x(t) + B_2 \cdot u(t)$
Output Vector	$y(t) = C \cdot \tilde{x}(t) + D \cdot u(t)$

Table 4 – State-space averaging equations.

## ii. Circuit Averaging

Likewise circuit averaging can also be applied to achieve similar results as state space averaging. In this case instead of averaging the system differential equations, the averaging process is applied to the “terminals” of a circuit “switch.” Figure 8 shows a buck converter with the portion of the circuit that is to be averaged highlighted.

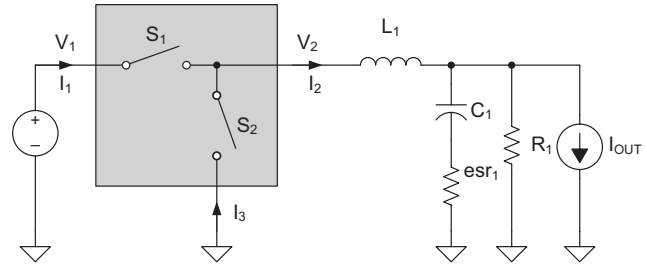


Figure 8 – Circuit averaging.

The averaging process works by averaging the values of  $I_1$ ,  $I_2$ ,  $V_1$  and  $V_2$  shown in Figure 8.

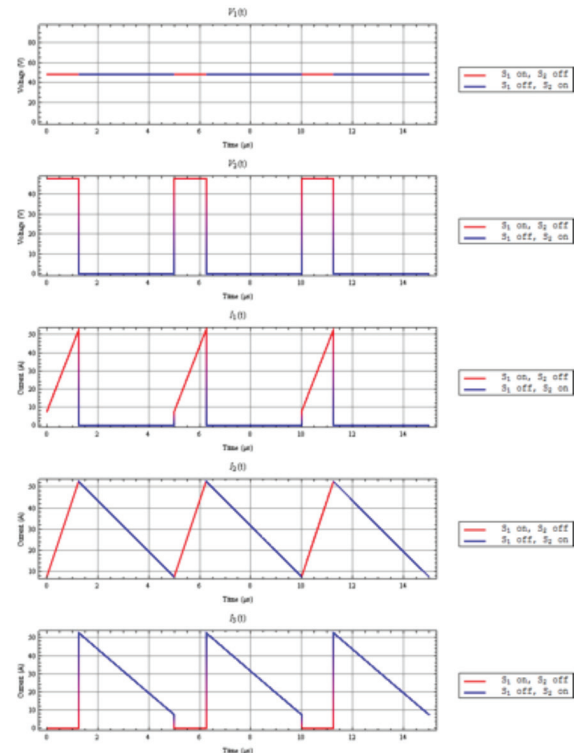


Figure 9 – Key waveforms for circuit averaging.

Both circuit-averaging and state-space-averaging work well when the method is able to consider only the effects of frequencies much lower than the switching frequency (e.g. buck-derived applications). This same concept cannot



be easily applied to the LLC converter. This stems from the fact that the LLC converter does not utilize a low-pass filter as much as it does a band-pass filter. In the case of a band-pass filter both low and high frequencies are rejected; therefore it becomes less obvious how to accomplish the averaging. Fundamentally, a method is required which captures the “average” behavior without rejecting the necessary frequency components of the system. Section iii describes this process.

### iii. Describing Functions

Describing functions are considered as a generic way to average the system’s states for each mode without losing any critical information contained in the system. A describing function operates by considering only specific frequency content of a given system. Any periodic continuous-time waveform can be represented by a summation of sine and cosine waves. Figure 10 illustrates the Fourier series expansion of a square wave. In the graph, the first three non-zero harmonics are shown. In this case it is the 1<sup>ST</sup>, 3<sup>RD</sup> and 5<sup>TH</sup>. If these three waveforms are added together the result begins to look like a square wave. The original square wave is reproduced to an arbitrary degree of accuracy simply by including more harmonics. However, in almost all cases, it only takes a few harmonics to accurately capture the salient features of the system.

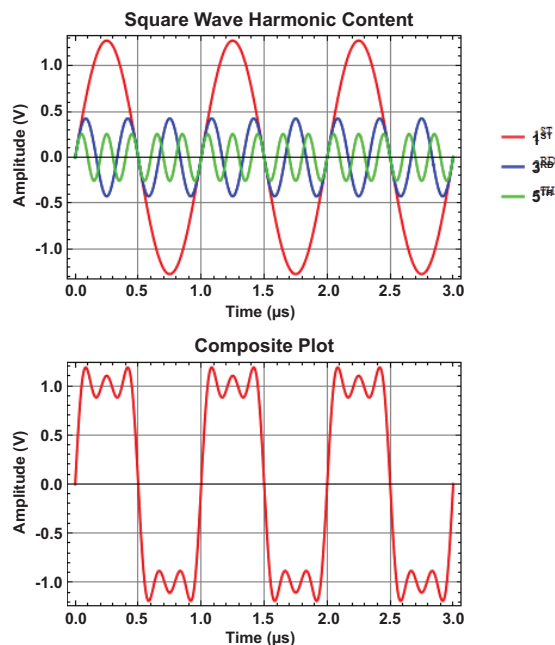


Figure 10 – Fourier series.

Figure 11 shows a simple block diagram for a non-linear system. If the input to this system is excited sinusoidally the output of the system has some significant non-linear effects; however, in the case of a power supply it also has a dominant linear response. This response is illustrated in Figure 12.

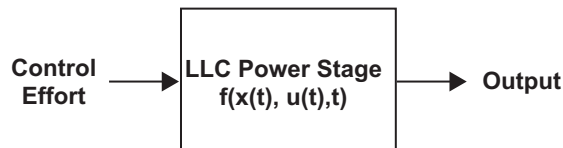


Figure 11 – Basic control system.

A Fourier series expansion applied to the non-linear output of this system results in a very good approximation of the system behavior. Care must always be employed in using a method like this in that excellent correlation, as is shown in Figure 12, does not always result. Fortunately for a power supply like the LLC converter it almost always does.

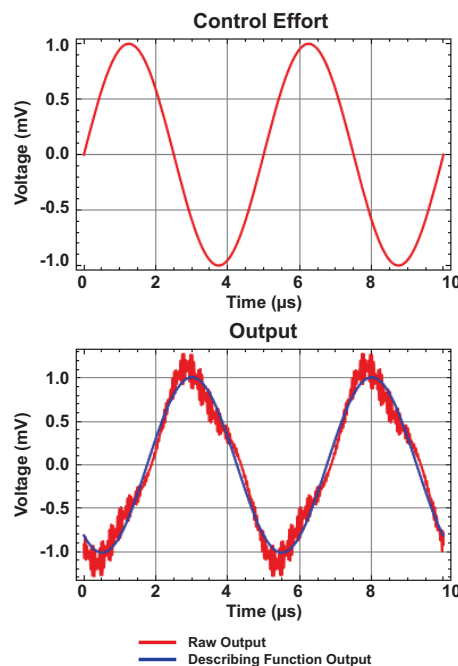


Figure 12 – Describing function method.

Figure 13 applies the Fourier series expansion to the actual state-variables of an LLC converter in the below-resonance operating mode. The wave forms for this mode are shown as well as the spectral content of each state-variable. From a

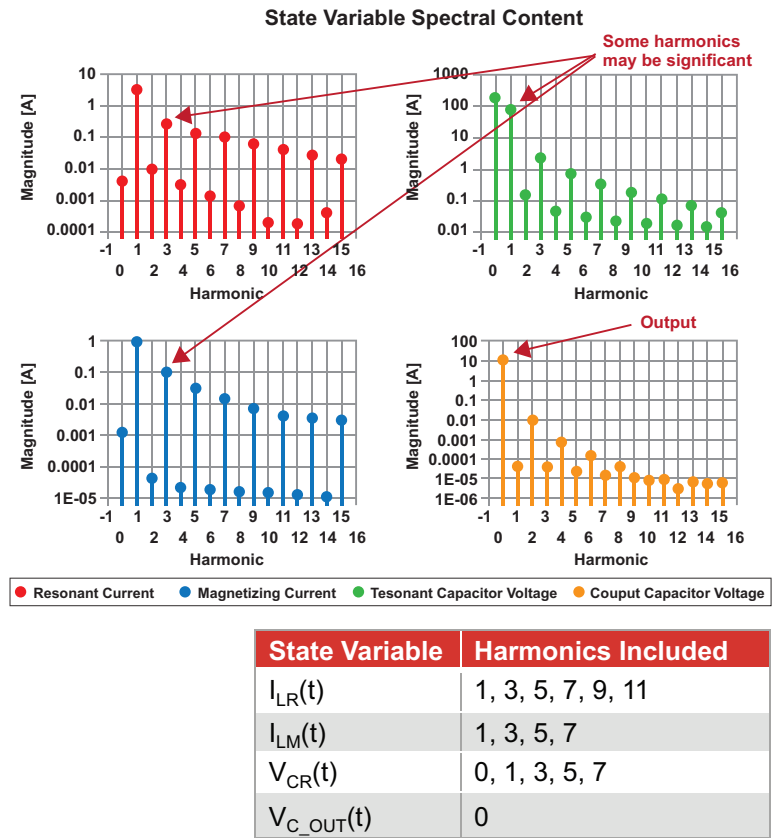
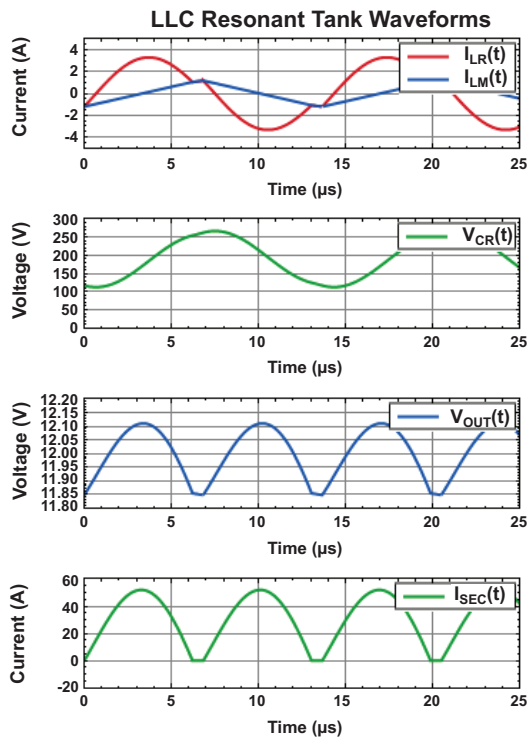


Figure 13 – Spectral considerations.

practical standpoint, the spectral content is derived using the discrete time Fourier transform rather than the Fourier series. By examining the magnitude of this content a designer can get a feel for which harmonics in the system are significant and, therefore, must be included in the subsequent application of the Fourier series expansion in the describing function process. In this case it was elected to use the harmonics shown in the figure. The resulting model is capable of including an arbitrary number of harmonics for each state-variable; however, this is limited to a more practical set that, in the opinion of the author, exceeds the requirements suggested by the data.

Each system state of the LLC converter is modeled by a linear system defined by the following equations. In this  $x(t)$  equation represents a vector of the system state-variables. For completeness the output vector  $y(t)$  is also shown.

$$\dot{x}(t) = A \cdot x(t) + B \cdot u(t)$$

$$y(t) = C \cdot x(t) + D \cdot u(t)$$

The actual system response, as has already been discussed, is actually non-linear and is represented by the following equations:

$$\dot{x}(t) = f(x(t), u(t), t)$$

$$y(t) = g(x(t), u(t), t)$$

By applying a Fourier series expansion to the entire operating mode the following equations result:

$$x^{ss}(t) = X_0^{ss} + \sum_{k=1}^{\infty} (X_{ck}^{ss} \cdot \cos(k \cdot \omega_s \cdot t) + X_{sk}^{ss} \cdot \sin(k \cdot \omega_s \cdot t))$$

$$F_{sk}^{ss} = \frac{2}{T_s} \cdot \sum_{i=1}^Q \int_{T_{i-1}}^{T_i} (A_i \cdot x(t)^{ss} + B_i \cdot U_0) \cdot \sin(k \cdot \omega_s \cdot t) \cdot dt$$

$$F_{ck}^{ss} = \frac{2}{T_s} \cdot \sum_{i=1}^Q \int_{T_{i-1}}^{T_i} (A_i \cdot x(t)^{ss} + B_i \cdot U_0) \cdot \cos(k \cdot \omega_s \cdot t) \cdot dt$$

$x^{ss}(t)$  is the steady-state value of the state variables,  $F_{sk}^{ss}$  and  $F_{ck}^{ss}$  are the sine and cosine coefficients of the non-linear function  $f(x(t), u(t), t)$  in steady state, and  $k$  is the  $k^{th}$  harmonic of the expansion.

## B. Linearization

The next step in the small-signal modelling process is to linearize the result. Linearization is illustrated in Figure 14.

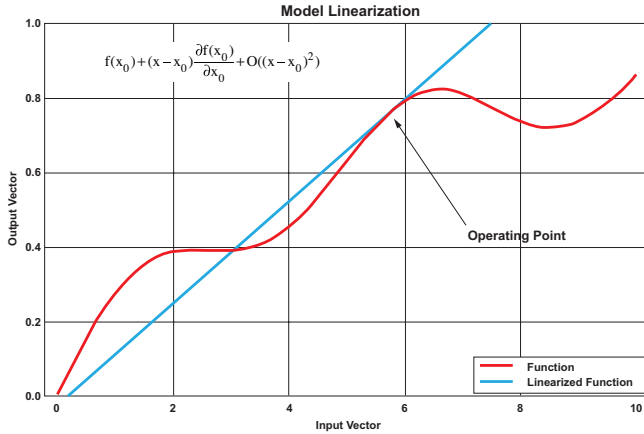


Figure 14 – Linearization.

The x-axis is the input to the system and the y-axis is the output. The red line shows an arbitrary, non-linear response. It is necessary to approximate the behavior of this line with a function that possesses the necessary attributes of a linear system. Those attributes are:

$$f(x_1 + x_2) = f(x_1) + f(x_2)$$

$$a \cdot f(x) = a \cdot f(a \cdot x)$$

Mathematically this can be accomplished by taking the Taylor series expansion of the function for the red-line about its operating point:

$$f(x) \cong f(x_0) + (x - x_0) \cdot \frac{\partial f(x_0)}{\partial x_0}$$

Since the describing function applied in the previous step was obtained in the form of an equation, a Taylor series expansion is directly applied to this result.

## C. Steady State Operating Point

The last piece of the puzzle required to obtain a meaningful result is the steady-state operating point. Unfortunately this is also a bit of a challenge for the LLC converter. A 2<sup>ND</sup> order system usually approximates a simple buck, boost or buck-boost converter well. Even if it is not 2<sup>ND</sup> order its steady state solution almost always is estimated by one. This fact makes it relatively easy to derive the steady state solution. The LLC converter is, by nature, a 4<sup>TH</sup> order system and, to-date, this author is not aware of a sufficiently accurate way to approximate the steady state behavior without simulation. Therefore, in order for this model to be practical, it is necessary to have a way to quickly and accurately calculate this operating point. In order to do this the concepts of state-variables, states and modes are exploited to come up with a simulator that is both very fast and extremely accurate.

Each system state in the LLC converter is approximated as a linear differential equation. Using linear algebra and the matrix-exponential function, a closed form solution to the differential equations in each state is obtained. Taking the final values of the state-variables and making them the initial conditions for the subsequent state in a given mode obtains a lightning-fast, highly accurate simulator. The basic equations for this algorithm are shown below:

$$\dot{x}_n(t) = A \cdot x_n(t) + B \cdot U$$

$$x_n(t_i) = (e^{A \cdot t} - I) \cdot A^{-1} \cdot B \cdot U + e^{A \cdot t} \cdot x_n(t_{i-1})$$

### III. MODEL VALIDATION

Figures 15 and 16 show two graphs that substantiate the accuracy of the resulting model. Figure 15 compares the model with an independent circuit simulation of an LLC converter with a high Q in the resonant tank.

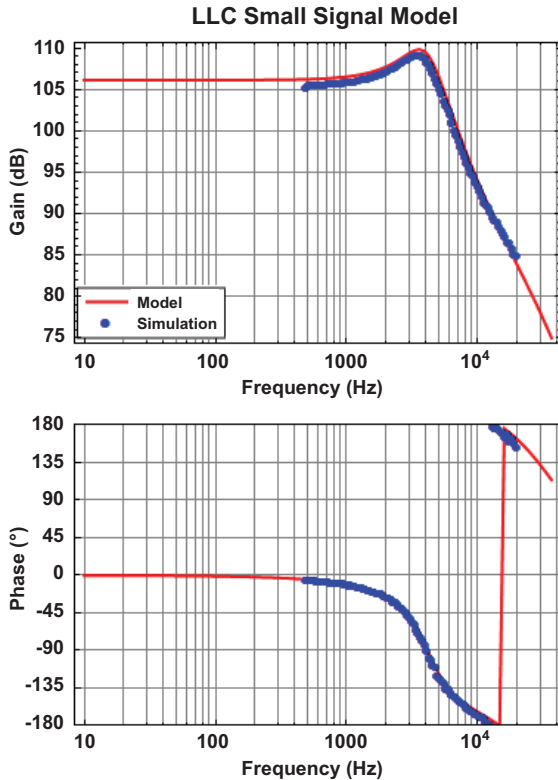


Figure 15 – Model vs. circuit simulation.

Figure 16 compares the model with physical lab measurements of an actual LLC converter.

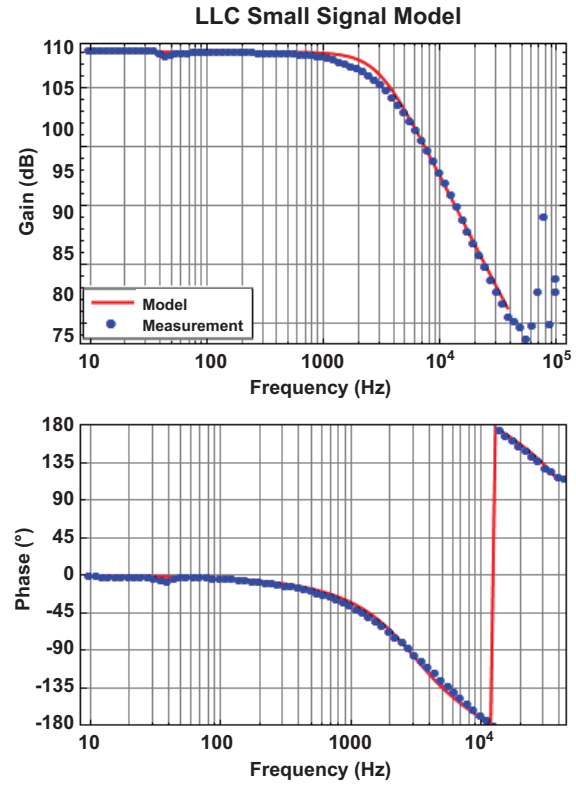


Figure 16 – Model vs. measurement.

In both cases the correlation is excellent and the results provide substantial evidence to the model's facility to accurately predict the LLC plant gain and phase.

### IV. CASE STUDY

#### A. Plant Analysis

In this section a discussion of practical implications for the LLC converter is discussed as well as an illustrative example of how to choose the appropriate compensation values and the resulting impacts of those choices. To begin, consider the LLC plant response shown in Figure 17.

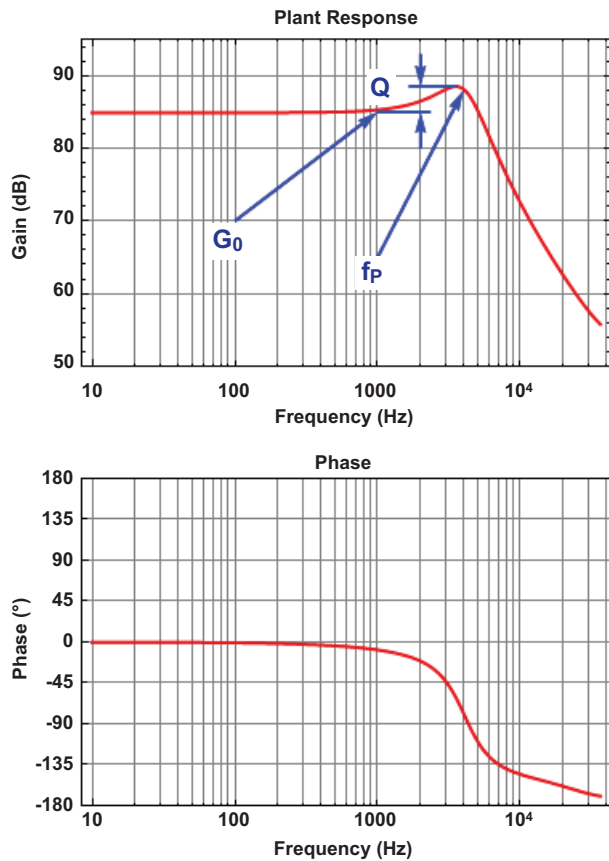


Figure 17 – Typical plant characteristics.

For starters, earlier in this paper it was stated that the LLC converter is a 4<sup>th</sup> order system; however, Figure 17 also illustrates that the dominate plant behavior is still 2<sup>nd</sup> order. In fact, some key information is also extracted from this plot that to help determine the numerical values of the required compensation. This data is listed in Table 5.

Symbol	Value	Description
$G_0$	85 dB	The low frequency gain, sometimes called the DC gain.
$Q$	1.35	The plant quality factor. This is a measure of the plant gain a resonance.
$f_P$	4 kHz	The plant resonant frequency.

Table 5 – Plant salient features.

## B. Compensation Objectives

Before discussing any details on how to compensate something, it is important to first understand the goals of the compensation. At a high level there are three fundamental goals: stability, reference tracking and disturbance

rejection. Stability all by itself is trivial. LLC converters are open-loop stable so they always start out stable. It is only after messing with them and doing things to improve the reference tracking and disturbance rejection that they become difficult to stabilize. Some typical power supply stability margins and their associated definitions are shown in Table 6.

Symbol and Value	Description
$\phi_m \geq 45^\circ$	Phase margin. This is the amount of phase change necessary to make the system unstable when the gain is exactly equal to 0 dB.
$g_m \geq 10$ dB	Gain margin. This is the amount of gain change necessary to make the system unstable when the phase is exactly equal to $0^\circ$ .

Table 6 – Stability objectives.

The goal of the compensation then becomes how to improve the reference tracking ability of the power supply and its corresponding disturbance rejection ability without destroying its inherent stability. This is a very real problem in that the open loop reference tracking and disturbance rejection ability are typically terrible.

## C. Compensation Process

The first thing that needs to be added to the system is an integrator in order to achieve ideal DC reference tracking. Once done, it will then be necessary to adjust the gain and add some additional poles and zeros to the system to achieve the best disturbance rejection ability possible. One metric of a systems ability to reject disturbances is the bandwidth. As a starting point consider the following compensator:

$$G_0 \cdot \frac{\frac{s^2}{(2 \cdot \pi \cdot f_Z)^2} + \frac{s}{2 \cdot \pi \cdot f_Z \cdot Q_Z} + 1}{s}$$

The  $\frac{1}{s}$  term is required to eliminate the DC error and the two zeros are utilized to reduce the phase shift caused by the three poles in the system to a value that allows us to maintain the stability margins shown in Table 6. Graphically this compensator is shown in Figure 18. In this case the two zeros of the system have been placed at

the same locations as the dominant plant poles and also utilize the same Q as the plant. The gain  $G_0$  is also adjusted so that it is easy to see the curves in Figure 18.

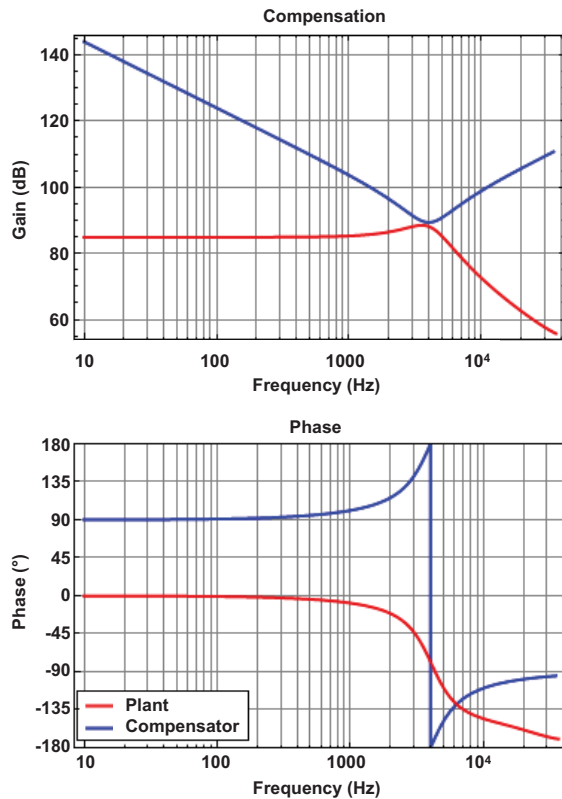


Figure 18 – Initial compensator.

Table 7 summarizes the initial compensation choices for this design. Figure 19 shows the resulting behavior.

Symbol	Value	Description
$G_0$	0 dB	The low frequency gain of the compensator. Sometimes called the DC gain.
$Q_z$	1.35	The compensator zero quality factor.
$f_z$	4 kHz	The position of the compensator's complex zero pair.

Table 7 – Initial compensation choices.

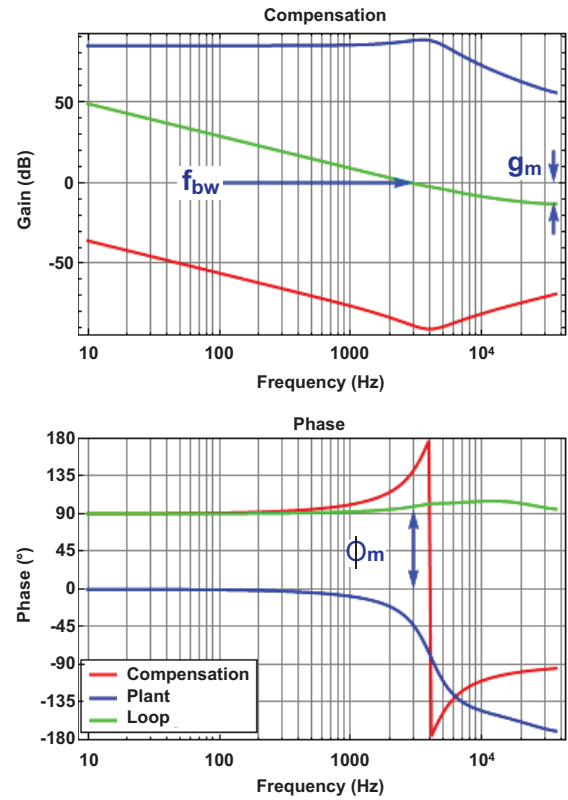


Figure 19 – Initial compensation choices.

The performance metrics of these compensation choices are listed in Table 8.

Symbol	Value	Description
$g_m$	12 dB	Gain margin. This is the amount of gain change necessary to make the system unstable when the phase is exactly equal to 0 °.
$\phi_m$	95 °	Phase margin. This is the amount of phase change necessary to make the system unstable when the gain is exactly equal to 0 dB.
$f_{bw}$	3 kHz	Bandwidth. This is the frequency of the system where the gain equals 0 dB. This is a figure of merit of the system's ability to reject disturbances.

Table 8 – Initial performance metrics.

While these values all meet the required stability objectives, adding an extra pole to the compensator achieves a significant improvement. The new compensator is shown below.

$$G_0 \cdot \frac{\frac{s^2}{(2 \cdot \pi \cdot f_z)^2} + \frac{s}{2 \cdot \pi \cdot f_z \cdot Q_z} + 1}{s \cdot \frac{s}{2 \cdot \pi \cdot f_p} + 1}$$



The values of the compensation parameters are summarized in Table 9.

Symbol	Value	Description
$G_0$	0 dB	The low frequency gain of the compensator. Sometimes called the DC gain.
$Q_z$	1.35	The compensator zero quality factor.
$f_z$	4 kHz	The position of the compensator's complex zero pair.
$f_p$	15 kHz	Extra compensator pole

Table 9 – Compensation choices with an extra pole.

Figure 20 shows the resulting Bode plot.

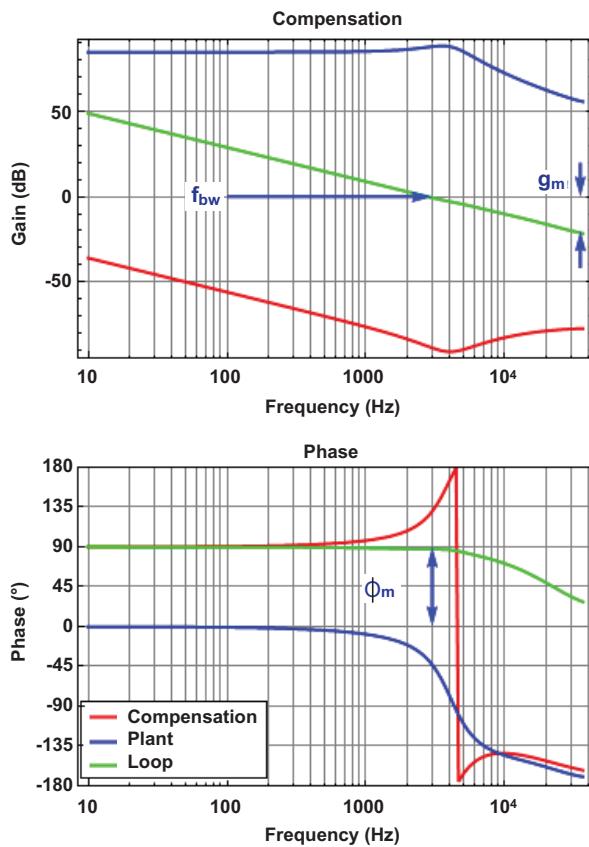


Figure 20 – Bode plot with an extra pole.

Table 10 summarizes the resulting performance metrics for these new compensation choices. Notice that there is little to no impact to the  $\phi_m$  or  $f_{bw}$ , however, there is a substantial improvement to  $g_m$ . The relevance of this improvement is shown in the subsequent sections.

Symbol	Value	Description
$g_m$	20 dB	Gain margin. This is the amount of gain change necessary to make the system unstable when the phase is exactly equal to 0 °.
$\phi_m$	90 °	Phase margin. This is the amount of phase change necessary to make the system unstable when the gain is exactly equal to 0 dB.
$f_{bw}$	3 kHz	Bandwidth. This is the frequency of the system where the gain equals 0 dB. This is a figure of merit of the system's ability to reject disturbances.

Table 10 – Performance metrics with  $G_0 = 9.5$  dB.

## D. Performance Considerations

The previous section only focused on eliminating the DC error inherent to the LLC converter without any serious consideration to how well it rejects system disturbances. While  $f_{bw}$  is a very useful metric, it is inadequate in its ability to quantify the benefits of one compensation choice versus another. In order to do this the closed-loop performance metrics that the system engineer cares about must be examined. Classically these are the output-impedance and the input-voltage-transient-rejection capability. The former is a measure of the system's ability to reject disturbances caused by load current variations, while the latter is a measure of the system's ability to reject input voltage variations.



### i. Output Impedance, $Z_{OUT}(s)$

Using the compensation choices summarized in Table 9 as a starting point, Figure 21 graphs the resulting compensation and  $Z_{OUT}(S)$ .

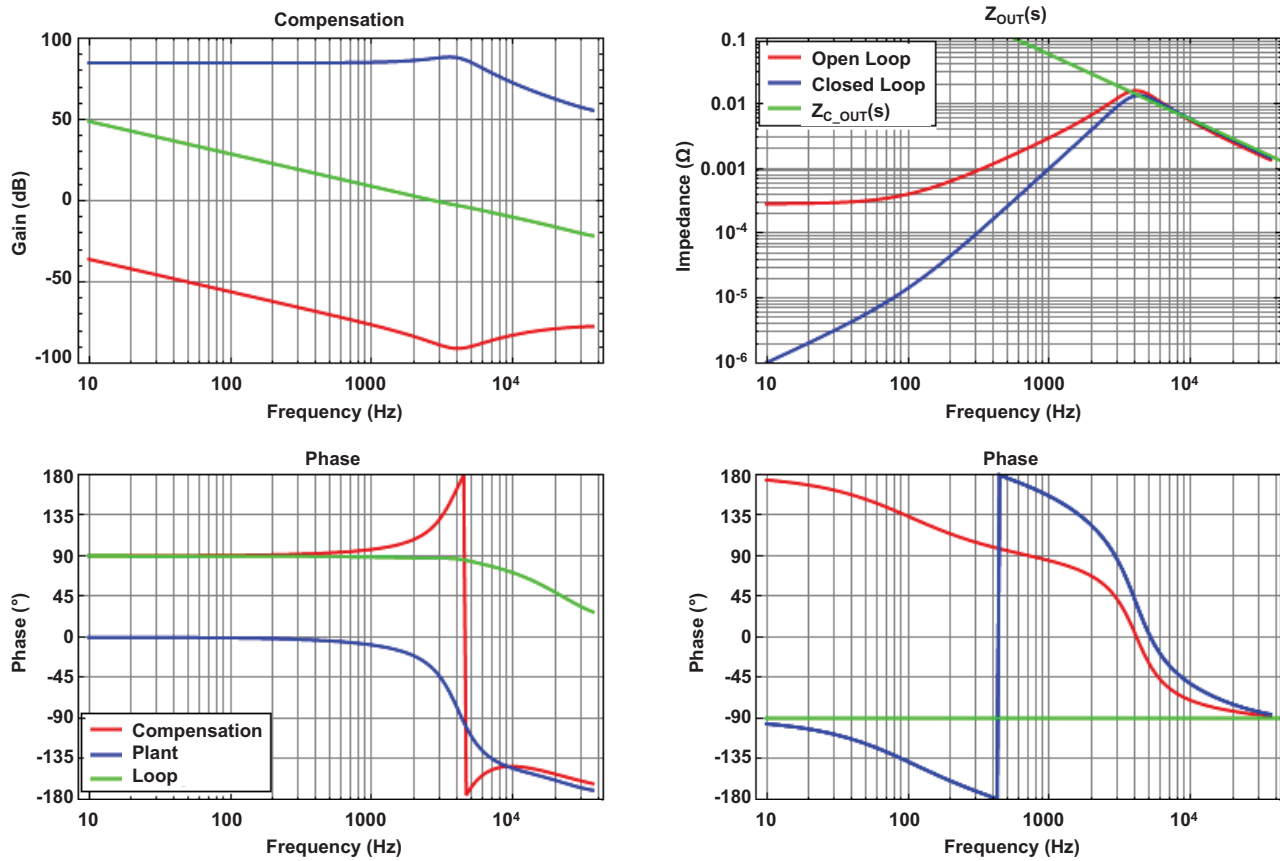


Figure 21 –  $Z_{OUT}(s)$ ,  $G_0 = 0$  dB.

Three curves are shown in order to illustrate the benefit the feedback (i.e. the compensation) provides to this transfer function.

Symbol	Description
$Z_{OUT}(s)$ , Open Loop	This is the open loop output impedance of the converter.
$Z_{OUT}(s)$ , Closed Loop	This is the closed loop output impedance of the converter.
$Z_{C\_OUT}(s)$	This is the impedance of the output capacitor bank. It is added as an additional metric to justify the accuracy of the model.

Table 11 –  $Z_{OUT}(s)$  curve descriptions.

Notice that the feedback provides a considerable reduction to  $Z_{OUT}(s)$ . This improvement is most notable at lower frequencies where the gain of the system is the largest. Once the frequency has crossed 0 dB the ability of the compensator to reject disturbances is diminished and the three curves converge.

In an effort to improve the performance, the gain of the compensator is increased from 0 dB to 9.5 dB. The resulting graphs are illustrated in Figure 22.

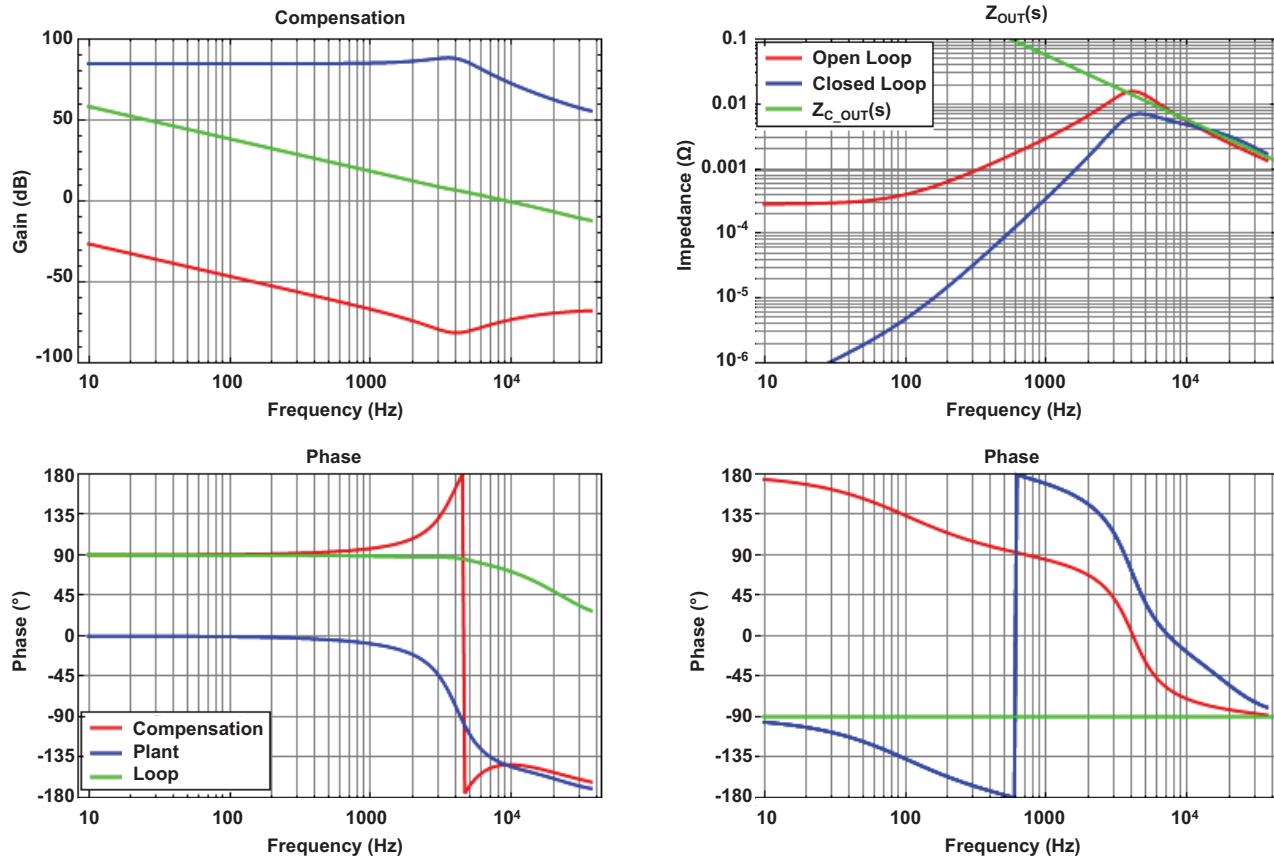


Figure 22 –  $Z_{OUT}(s)$ ,  $G_0 = 9.5$  dB.

Under this new compensation there is considerable improvement, i.e. reduction in  $Z_{OUT}(s)$ . Table 12 summarizes the new stability metrics. Notice that the bandwidth is significantly improved without an appreciable degradation in the corresponding stability margins.

Symbol	Value	Description
$g_m$	15 dB	Gain margin. This is the amount of gain change necessary to make the system unstable when the phase is exactly equal to 0 °.
$\phi_m$	70 °	Phase margin. This is the amount of phase change necessary to make the system unstable when the gain is exactly equal to 0 dB.
$f_{bw}$	10 kHz	Bandwidth. This is the frequency of the system where the gain equals 0 dB. This is a figure of merit of the system's ability to reject disturbances.

Table 12 – Performance metrics with an extra pole.

**ii. Input Voltage Disturbance Rejection,**  
 $\hat{V}_{OUT}(s)/\hat{V}_{IN}(s)$

The process taken in section i is now repeated for  $\hat{V}_{OUT}(s)/\hat{V}_{IN}(s)$ . As before, the compensation

choices summarized in Table 9 are the starting point and Figure 23 graphs the resulting compensation and  $\hat{V}_{OUT}(s)/\hat{V}_{IN}(s)$ .

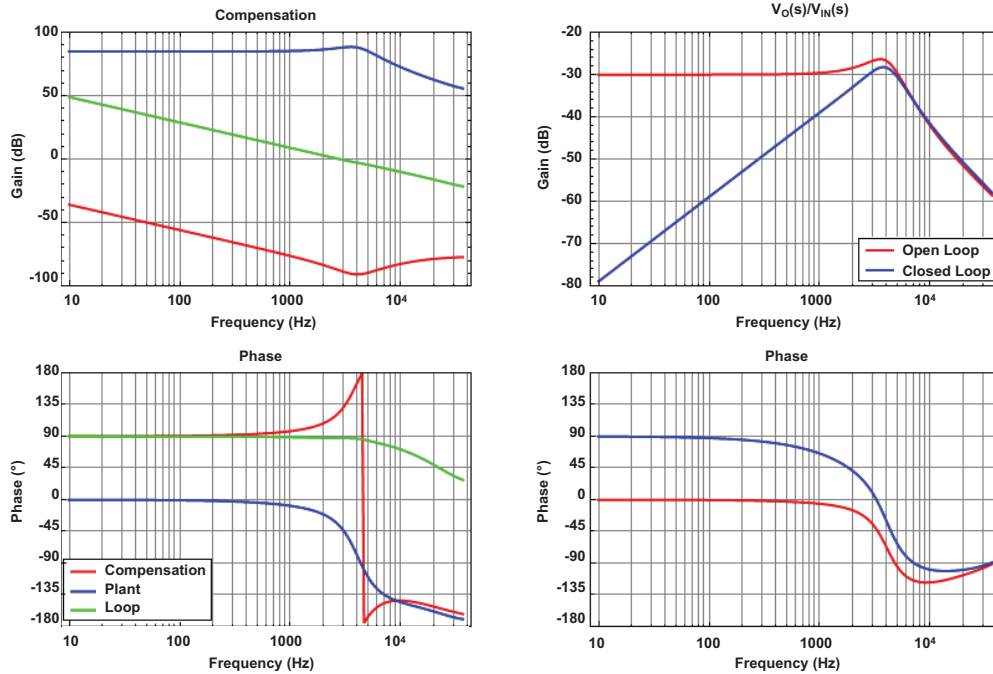


Figure 23 –  $\hat{V}_{OUT}(s)/\hat{V}_{IN}(s)$ ,  $G_0 = 0$  dB.

The feedback, again, provides a considerable reduction in the  $\hat{V}_{OUT}(s)/\hat{V}_{IN}(s)$  transfer function. Next, the gain of the compensator is increased from 0 dB to 9.5 dB. The resulting graphs are illustrated in Figure 24.

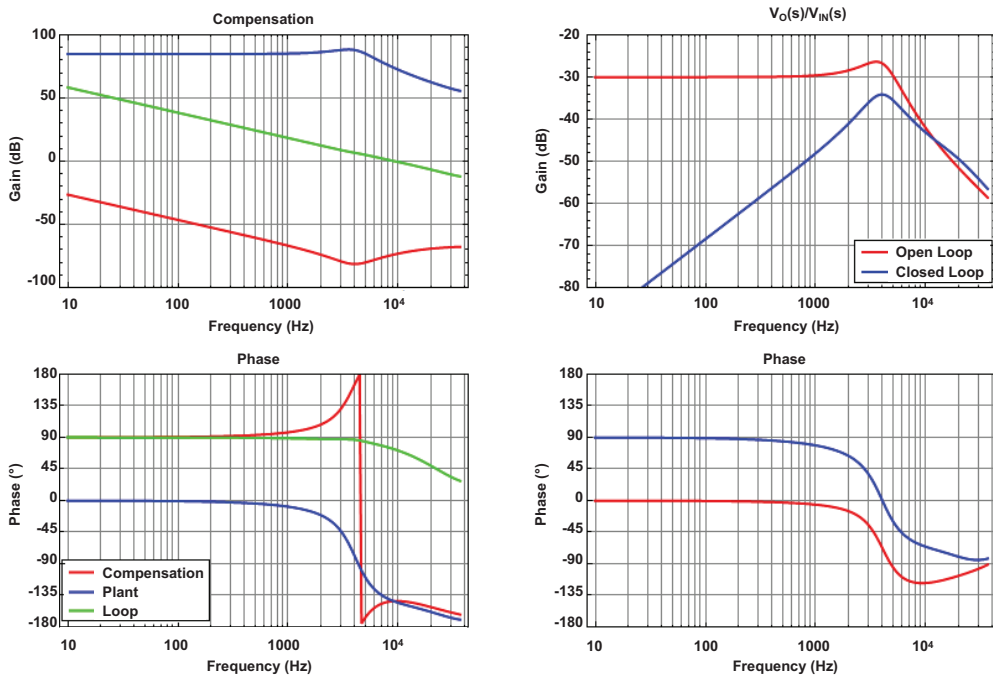


Figure 24 –  $\hat{V}_{OUT}(s)/\hat{V}_{IN}(s)$ ,  $G_0 = 9.5$  dB.

As before, the system now has a greater capability to reject input voltage variations without appreciable degradation in the stability margins.

## E. Plant Variations

In order to finish off the discussion of the small signal model, it is valuable to discuss how the plant characteristics change with operating point. In this context, the operating point includes variations in input voltage as well as load. The word variation refers only to a shift in the DC operating point of the system and not small signal amplitude.

Figures 25 and 26 help to illustrate how these variations behave. Figure 25 shows two input voltages and the corresponding Bode plots for an array of different gains. When operating at 370 V all the load conditions represent the below-resonance operating mode. Operation at 400 V represents the above-resonance mode. Likewise Figure 26 shows the same kind of trends. In this case, two load conditions are considered over a range of input voltages. In all cases the solid lines represent operation at or below-resonance, while the dashed lines are above-resonance.

Operation at or below-resonance appears as a second order system. The overall dynamics are approximately independent of the load and input

voltage operating point. This seems to match the intuition of the circuit. At resonance the tank is thought of as a short circuit, removing any load dependence. In addition, when the input voltage falls, the system still operates at the resonant frequency with dead times between  $\frac{1}{2}$  cycles. These dead times (i.e. time periods when the synchronous rectifiers do not conduct) produce a greater variation in the voltage across the resonant capacitor which ultimately increases the “gain” of the system. Presumably these dead times are what give the system its input voltage independent appearance. This is also observed in the DC operating point curves.

Operation above-resonance results in significantly more variation in the Bode plots. There is a strong dependence on load. In addition it appears that the transition from the resonant frequency mode to the above-resonant mode results in the system poles splitting from a complex pole pair into two real poles. This could be the result of the fact that when operating below-resonance there are two distinct states. There are four actually, but two of them are just a mirror

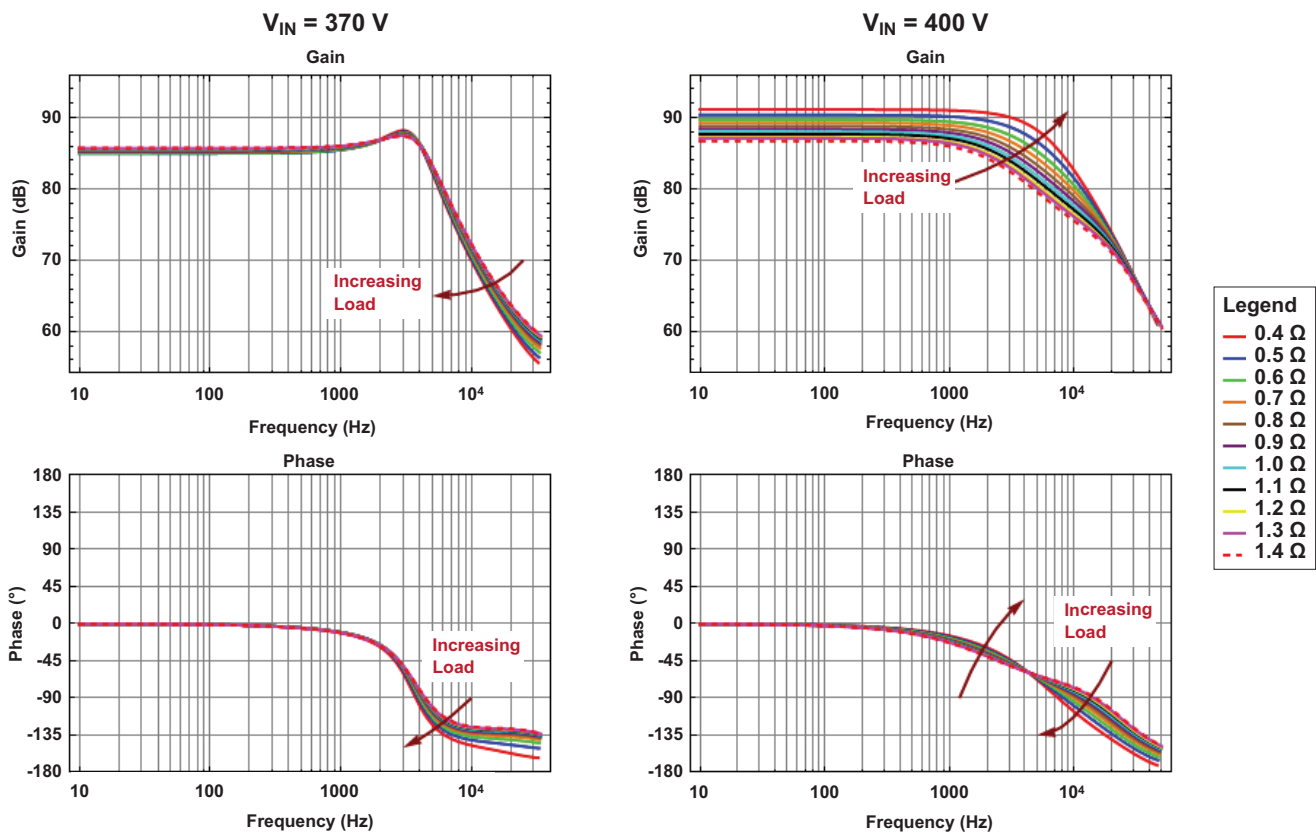


Figure 25 – Load variation.

image of the other two. However, there is only one state that transfers energy. When operating above-resonance there are still only two states (again, actually four) but, in this case, both states transfer energy. This author suspects that it is the ratio of these two modes to the overall energy transfer cycle that creates more drastic plot variations.

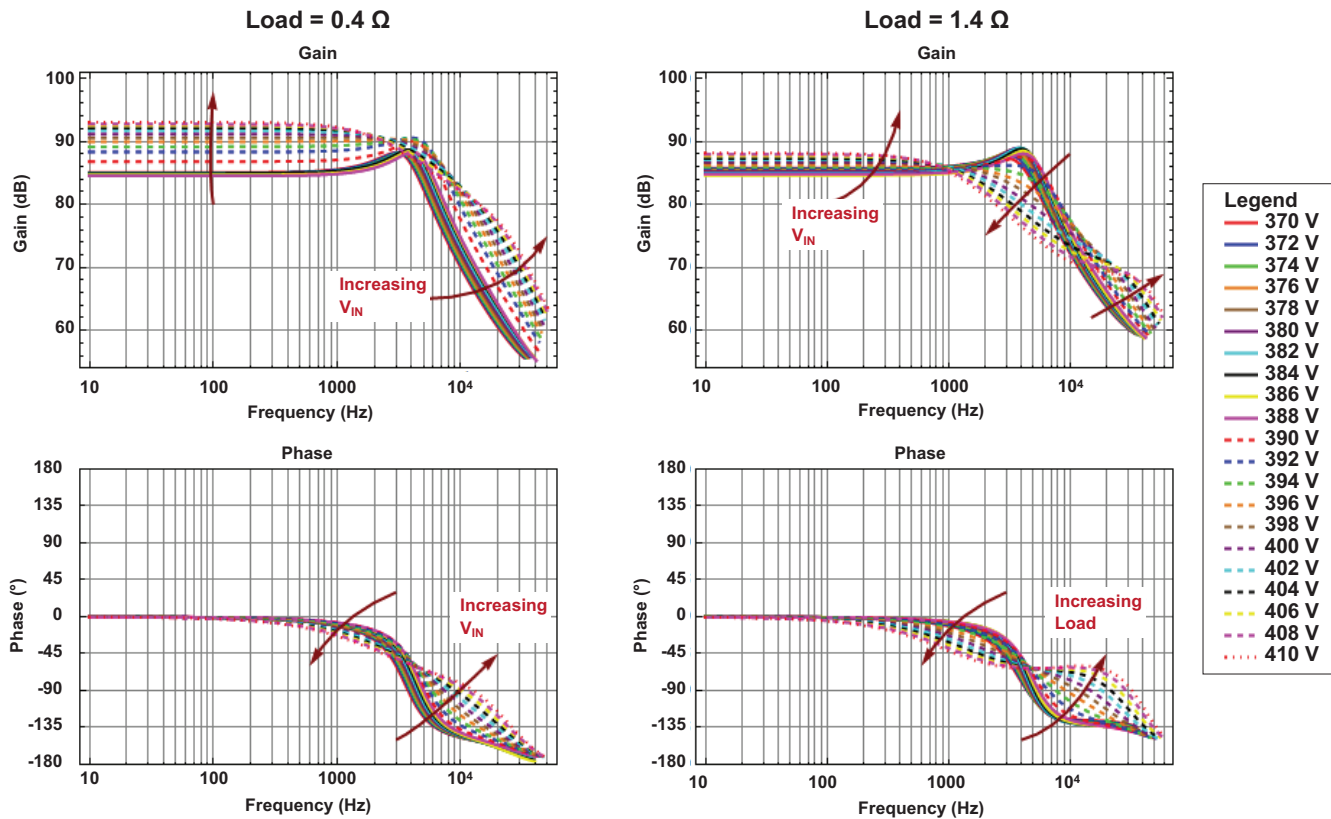


Figure 26 –  $V_{IN}$  variation.

## V. OVERVIEW OF KEY TOOLS ENABLING THE PRACTICAL USE OF THE NEW MODEL

The complexity of the new model prohibits wide spread use and adoption without some kind of aid. Therefore, a set of GUI based tools have been developed to make the application of the model trivial to a wide variety of operating conditions. This tool is packaged with the Fusion Digital Power Designer. By doing this, users are provided with a turn-key environment to both analyze and program their loop coefficients.

Figure 27 shows a screen shot of the design tab

of the Fusion Digital Power Designer. For those readers not familiar with this tool, it is a turn-key environment for working with the UCD based digital power products from Texas Instruments. The new LLC based tools provide small signal modeling support for both half-bridge and full-bridge LLC configurations as well as an easy-to-use format that allows users to customize the component values used in their application. The small signal model automatically analyzes the system and determines the operating mode as well as the unique operating states used in that mode. While this paper only discussed three operating modes, this tool is not limited to that.



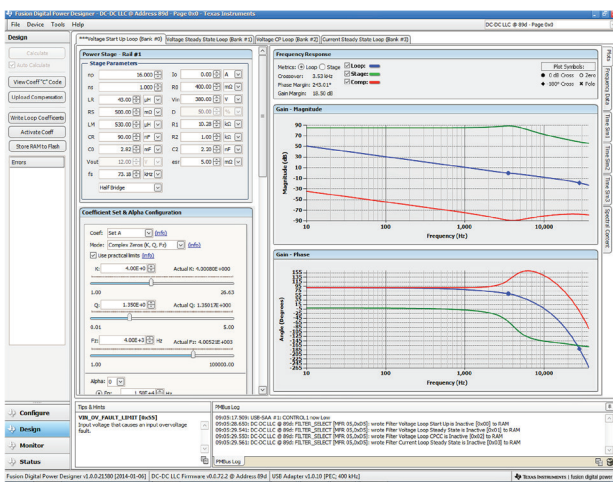


Figure 27 – Fusion design tab.

In addition to the small signal model discussed, the steady state operating point finder also provides a wide array of outputs that give the user additional insight into the operation of the specific LLC converter under consideration. Figures 28 and 29 show some examples of the kinds of plots that are available. If a new component value is selected, the Bode plot, associated time domain data, frequency domain, states and modes are all recalculated and the GUI display is updated in just a couple of seconds. This fast accurate response makes these tools an incredibly valuable design aid to the power supply designer's tool box.

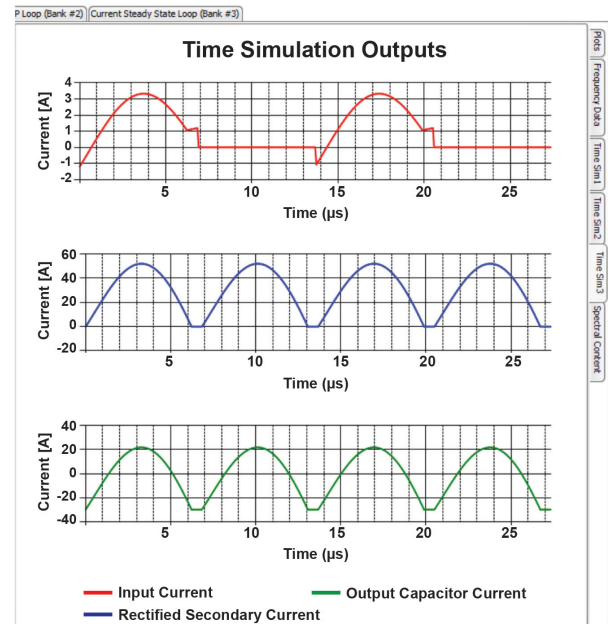


Figure 29 – Fusion secondary currents.

## VI. PRACTICAL LIMITATIONS

While great effort has been taken to validate the results of the model and the associated outputs, there are still some limitations, as one might expect from any such model. For starters, a model like this is only going to give predictions commensurate with the inputs provided. In other words, if the input parameters are not correct the output cannot be expected to be correct. On top of this there are a few other scenarios where the user should exercise caution before trusting the results:

- Low efficiency scenarios may need additional work to achieve proper correlation. At very low efficiency the loss terms in the real circuit may be large enough that the model does not predict the correct behavior. It may be possible to compensate for this by increasing the model resistance.
- The model does not support PWM or PSM. The model was created with the infrastructure to support these modulation methods. Texas Instruments is interested in hearing from companies and designers who have an interest in PWM and PSM modulation methods being included in this model.

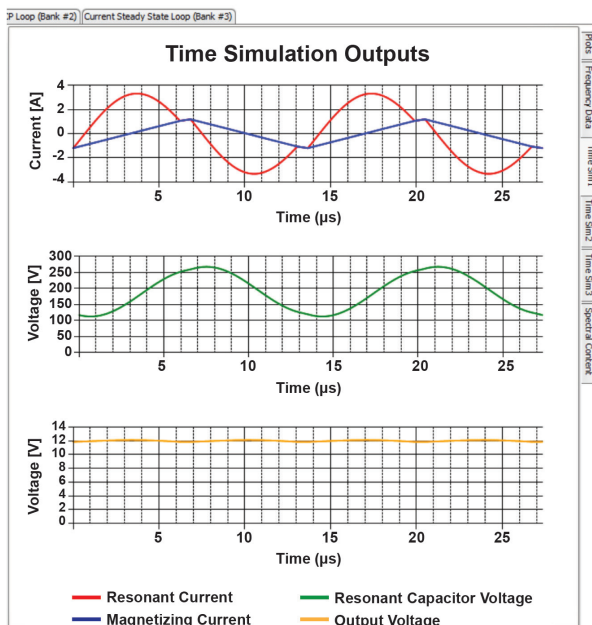


Figure 28 – Fusion resonant current.

- Corner cases may exist which limit the accuracy due to numerical approximations.
- Additional work may be required to ensure accuracy, especially at higher frequencies.
- Higher frequency operation may include the effects of parasitics that were not considered during the original modelling process.

## VII. CONCLUSIONS & FUTURE WORK

A new set of modelling methods and tools have been presented which are capable of predicting the small and large signal behavior of the LLC converter for virtually any operating mode. This tool set provides the design engineer with analytical predictions of plant pole zero behavior that enables more robust compensation as well as the ability to simulate and predict parameter variations & extreme operating conditions. In addition, it provides independent validation of the DC operating point along with instant visualization of key system waveforms and harmonic content. All of this is provided with seamless integration to TI standard isolated digital controllers.

This new tool set opens a wide variety of other features that can be added into future version of the GUI. Among these features are:

- DC operating point plots based on time domain simulation instead of just the first harmonic approximation.
- Performance metric plots like:
  - $Z_{OUT}(s) = \hat{V}_{OUT}(s) / \hat{I}_{OUT}(s)$
  - $Z_{IN}(s) = \hat{V}_{IN}(s) / \hat{I}_{IN}(s)$
  - $\hat{V}_{OUT}(s) / \hat{V}_{IN}(s)$
  - $\hat{I}_{IN}(s) / \hat{I}_{OUT}(s)$
- Additional modulation methods:
  - PSM
  - PWM
- Additional states & modes to include effects like:
  - Switching transitions
  - Body diode conduction

## VIII. REFERENCES

- [1] <http://www.plugloadsolutions.com/80PlusPowerSupplies.aspx>.
- [2] McDonald, Brent and Freeman, Dave, "Designing an LLC Resonant Half-Bridge Power Converter," SEM2000; Texas Instruments, Dallas, TX, 2012.
- [3] <http://www.ti.com/product/ucd3138>.
- [4] Yang, B., Lee, F.C. and Concannon, M., "Over Current Protection Methods for LLC Resonant Converter," Applied Power Electronics Conference and Exposition, 2003. APEC '03. Eighteenth Annual IEEE , vol.2, pp.605-609, Feb. 9-13, 2003.
- [5] Huang, Hong, "Designing an LLC Resonant Half-Bridge Power Converter," SEM1900; Texas Instruments, Manchester, NH, 2010.
- [6] Bing Lu; Wenduo Liu; Yan Liang; Lee, F.C.; van Wyk, J.D., "Optimal Design Methodology for LLC Resonant Converter," Applied Power Electronics Conference and Exposition, 2006. APEC '06. Twenty-First Annual IEEE, March 19-23, 2006.
- [7] Ya Liu; "High Efficiency Optimization of LLC Resonant Converter for Wide Load Range," Virginia Polytechnic Institute and State University, Master's Thesis, 2007.
- [8] Yiqing Ye; Chao Yan; Jianhong Zeng; Jianping Ying; "A Novel Light Load Solution for LLC Series Resonant Converter," Telecommunications Energy Conference, 2007. INTELEC 2007. 29th International, pp.61-65, Sept. 30 2007-Oct. 4 2007.
- [9] Maksimovic, D., Erickson, R., Griesbach, C, "Modeling of Cross-Regulation in Converters Containing Coupled Inductors," Applied Power Electronics Conference and Exposition, 1998. APEC '98. Conference Proceedings 1998, Thirteenth Annual, vol.1, pp.350-356, Feb 15-19, 1998.
- [10] Suntio, T., Glad, A., Waltari, P., "Constant-Current vs. Constant-Power Protected Rectifier as a DC UPS System's Building Block," Telecommunications Energy Conference, 1996. INTELEC '96, 18th International, pp.227-233, Oct 6-10, 1996.



- [11] Lazar, J.F., Martinelli, R., "Steady-State Analysis of the LLC Series Resonant Converter," Applied Power Electronics Conference and Exposition, 2001. APEC 2001. Sixteenth Annual IEEE, vol.2, pp.728-735, 2001.
- [12] Martin Zhang (Zhang Tao), Sober Hu (Hu Yanshen); "Phase Shifted Full Bridge LLC Resonant Converter", Web-Link.
- [13] <http://www.synopsys.com/Systems/Saber/Pages/default.aspx>.
- [14] <http://www.simatrix.co.uk/site/products/simplis.htm>.
- [15] R. D. Middlebrook, "Measurement of Loop Gain in Feedback Systems," Int. J. Electronics, 1975, pp. 485-512.
- [16] Groves, J.O. and Lee, F.C., "Small Signal Analysis of Systems with Periodic Operating Trajectories," Proc. VPEC Annual Seminar, 1988, pp. 224-235.
- [17] J. O. Groves, "Small-Signal Analysis Using Harmonic Balance Methods," Proc. IEEE PESC, 1991, pp. 74-79.
- [18] J. O. Groves, "Small-Signal Analysis of Nonlinear Systems with Periodic Operation Trajectories," Ph.D. Dissertation, Virginia Tech, Blacksburg, VA, April 1995.
- [19] E. Yang, "Extended Describing Function Method for Small-Signal Modeling of Switching Power Circuit," Proc. VPEC Annual Seminar, 1994, pp.87-96.
- [20] Yang, E., Lee, F.C. and Jovanovic, M., "Small-Signal Modeling of Series and Parallel Resonant Converters," Proc. IEEE APEC, 1992, pp. 785-792.
- [21] E. Yang, "Extended Describing Function Method for Small-Signal Modeling of Resonant and Multi-Resonant Converters," Dissertation, Virginia Tech, Blacksburg, VA, February 1994.
- [22] Wong, R. and Groves, J.O., "An Automated Small-Signal Frequency-Domain Analyzer for General Periodic-Operating Systems as Obtained via Time-Domain Simulation," Proc. IEEE PESC, 1995, pp. 801-808.
- [23] B. Yang, "Topology Investigation for Front End DC/DC Power Conversion for Distributed Power System," Dissertation, Virginia Tech, Blacksburg, VA, September 2003.
- [24] Yang, B. and Lee, F.C., "Small Signal Analysis for LLC Resonant Converter," Virginia Tech, Blacksburg, VA, 2002.
- [25] Hsiao, C., Ridley, R.B. and Lee, F.C., "The Simulation of Switching Converters Using the New Version COSMIR. Program," VPEC Seminar, September 1989.
- [26] Hsiao, C., Ridley, R.B., Naitoh, H. and Lee, F.C., "Circuit-Oriented Discrete-Time Modeling and Simulation for Switching Converters," IEEE Power Electronics Specialists Conference and Exposition, 1987.
- [27] Hsiao, C., Ridley, R.B. and Lee, F.C., "Small-Signal Analysis of Switching DC-DC Converters Using the Simulation Program COSMIR," VPEC Seminar, September 1988.
- [28] Witulski, A., Hernandez, A.F., Erickson, R.W., "Small Signal Equivalent Circuit Modeling of Resonant Converters," Power Electronics, IEEE Transactions on , vol.6, no.1, pp.11-27, Jan 1991.
- [29] V. Vorperian, "Approximate Small-Signal Analysis of the Series and the Parallel Resonant Converters," Power Electronics, IEEE Transactions on, Volume: 4, Issue: 1 , Jan. 1989.
- [30] Forsyth, A., Ho, Y.K.E., Ong, H.M., "Comparison of Small-Signal Modeling Techniques for the Series-Parallel Resonant Converter," Power Electronics and Variable-Speed Drives, Fifth International Conference on, 1994.
- [31] Sanders, S., Noworolski, J.M., Liu, X.Z. and Verghese, G.C., "Generalized Averaging Method for Power Conversion Circuits," IEEE PESC 1990.

# TI Worldwide Technical Support

---

## Internet

### TI Semiconductor Product Information Center Home Page

[support.ti.com](http://support.ti.com)

### TI E2E™ Community Home Page

[e2e.ti.com](http://e2e.ti.com)

## Product Information Centers

<b>Americas</b>	Phone	+1(512) 434-1560
<b>Brazil</b>	Phone	0800-891-2616
<b>Mexico</b>	Phone	0800-670-7544
	Fax	+1(972) 927-6377
	Internet/Email	<a href="http://support.ti.com/sc/pic/americas.htm">support.ti.com/sc/pic/americas.htm</a>

### Europe, Middle East, and Africa

Phone	
European Free Call	00800-ASK-TEXAS (00800 275 83927)
International	+49 (0) 8161 80 2121
Russian Support	+7 (4) 95 98 10 701

**Note:** The European Free Call (Toll Free) number is not active in all countries. If you have technical difficulty calling the free call number, please use the international number above.

Fax	+ (49) (0) 8161 80 2045
Internet	<a href="http://www.ti.com/asktexas">www.ti.com/asktexas</a>
Direct Email	<a href="mailto:asktexas@ti.com">asktexas@ti.com</a>

### Japan

Phone	Domestic	0120-92-3326
Fax	International	+81-3-3344-5317
	Domestic	0120-81-0036
Internet/Email	International	<a href="http://support.ti.com/sc/pic/japan.htm">support.ti.com/sc/pic/japan.htm</a>
	Domestic	<a href="http://www.tij.co.jp/pic">www.tij.co.jp/pic</a>

### Asia

Phone Toll-Free Number  
**Note:** Toll-free numbers may not support mobile and IP phones.

Australia	1-800-999-084
China	800-820-8682
Hong Kong	800-96-5941
India	000-800-100-8888
Indonesia	001-803-8861-1006
Korea	080-551-2804
Malaysia	1-800-80-3973
New Zealand	0800-446-934
Philippines	1-800-765-7404
Singapore	800-886-1028
Taiwan	0800-006800
Thailand	001-800-886-0010

International	+86-21-23073444
Fax	+86-21-23073686
Email	<a href="mailto:tiasia@ti.com">tiasia@ti.com</a> or <a href="mailto:ti-china@ti.com">ti-china@ti.com</a>
Internet	<a href="http://support.ti.com/sc/pic/asia.htm">support.ti.com/sc/pic/asia.htm</a>

**Important Notice:** The products and services of Texas Instruments Incorporated and its subsidiaries described herein are sold subject to TI's standard terms and conditions of sale. Customers are advised to obtain the most current and complete information about TI products and services before placing orders. TI assumes no liability for applications assistance, customer's applications or product designs, software performance, or infringement of patents. The publication of information regarding any other company's products or services does not constitute TI's approval, warranty or endorsement thereof.

A012014

The platform bar and E2E are trademarks of Texas Instruments. All other trademarks are the property of their respective owners.

## IMPORTANT NOTICE

Texas Instruments Incorporated and its subsidiaries (TI) reserve the right to make corrections, enhancements, improvements and other changes to its semiconductor products and services per JESD46, latest issue, and to discontinue any product or service per JESD48, latest issue. Buyers should obtain the latest relevant information before placing orders and should verify that such information is current and complete. All semiconductor products (also referred to herein as "components") are sold subject to TI's terms and conditions of sale supplied at the time of order acknowledgment.

TI warrants performance of its components to the specifications applicable at the time of sale, in accordance with the warranty in TI's terms and conditions of sale of semiconductor products. Testing and other quality control techniques are used to the extent TI deems necessary to support this warranty. Except where mandated by applicable law, testing of all parameters of each component is not necessarily performed.

TI assumes no liability for applications assistance or the design of Buyers' products. Buyers are responsible for their products and applications using TI components. To minimize the risks associated with Buyers' products and applications, Buyers should provide adequate design and operating safeguards.

TI does not warrant or represent that any license, either express or implied, is granted under any patent right, copyright, mask work right, or other intellectual property right relating to any combination, machine, or process in which TI components or services are used. Information published by TI regarding third-party products or services does not constitute a license to use such products or services or a warranty or endorsement thereof. Use of such information may require a license from a third party under the patents or other intellectual property of the third party, or a license from TI under the patents or other intellectual property of TI.

Reproduction of significant portions of TI information in TI data books or data sheets is permissible only if reproduction is without alteration and is accompanied by all associated warranties, conditions, limitations, and notices. TI is not responsible or liable for such altered documentation. Information of third parties may be subject to additional restrictions.

Resale of TI components or services with statements different from or beyond the parameters stated by TI for that component or service voids all express and any implied warranties for the associated TI component or service and is an unfair and deceptive business practice. TI is not responsible or liable for any such statements.

Buyer acknowledges and agrees that it is solely responsible for compliance with all legal, regulatory and safety-related requirements concerning its products, and any use of TI components in its applications, notwithstanding any applications-related information or support that may be provided by TI. Buyer represents and agrees that it has all the necessary expertise to create and implement safeguards which anticipate dangerous consequences of failures, monitor failures and their consequences, lessen the likelihood of failures that might cause harm and take appropriate remedial actions. Buyer will fully indemnify TI and its representatives against any damages arising out of the use of any TI components in safety-critical applications.

In some cases, TI components may be promoted specifically to facilitate safety-related applications. With such components, TI's goal is to help enable customers to design and create their own end-product solutions that meet applicable functional safety standards and requirements. Nonetheless, such components are subject to these terms.

No TI components are authorized for use in FDA Class III (or similar life-critical medical equipment) unless authorized officers of the parties have executed a special agreement specifically governing such use.

Only those TI components which TI has specifically designated as military grade or "enhanced plastic" are designed and intended for use in military/aerospace applications or environments. Buyer acknowledges and agrees that any military or aerospace use of TI components which have **not** been so designated is solely at the Buyer's risk, and that Buyer is solely responsible for compliance with all legal and regulatory requirements in connection with such use.

TI has specifically designated certain components as meeting ISO/TS16949 requirements, mainly for automotive use. In any case of use of non-designated products, TI will not be responsible for any failure to meet ISO/TS16949.

### Products

Audio	<a href="http://www.ti.com/audio">www.ti.com/audio</a>
Amplifiers	<a href="http://amplifier.ti.com">amplifier.ti.com</a>
Data Converters	<a href="http://dataconverter.ti.com">dataconverter.ti.com</a>
DLP® Products	<a href="http://www.dlp.com">www.dlp.com</a>
DSP	<a href="http://dsp.ti.com">dsp.ti.com</a>
Clocks and Timers	<a href="http://www.ti.com/clocks">www.ti.com/clocks</a>
Interface	<a href="http://interface.ti.com">interface.ti.com</a>
Logic	<a href="http://logic.ti.com">logic.ti.com</a>
Power Mgmt	<a href="http://power.ti.com">power.ti.com</a>
Microcontrollers	<a href="http://microcontroller.ti.com">microcontroller.ti.com</a>
RFID	<a href="http://www.ti-rfid.com">www.ti-rfid.com</a>
OMAP Applications Processors	<a href="http://www.ti.com/omap">www.ti.com/omap</a>
Wireless Connectivity	<a href="http://www.ti.com/wirelessconnectivity">www.ti.com/wirelessconnectivity</a>

### Applications

Automotive and Transportation	<a href="http://www.ti.com/automotive">www.ti.com/automotive</a>
Communications and Telecom	<a href="http://www.ti.com/communications">www.ti.com/communications</a>
Computers and Peripherals	<a href="http://www.ti.com/computers">www.ti.com/computers</a>
Consumer Electronics	<a href="http://www.ti.com/consumer-apps">www.ti.com/consumer-apps</a>
Energy and Lighting	<a href="http://www.ti.com/energy">www.ti.com/energy</a>
Industrial	<a href="http://www.ti.com/industrial">www.ti.com/industrial</a>
Medical	<a href="http://www.ti.com/medical">www.ti.com/medical</a>
Security	<a href="http://www.ti.com/security">www.ti.com/security</a>
Space, Avionics and Defense	<a href="http://www.ti.com/space-avionics-defense">www.ti.com/space-avionics-defense</a>
Video and Imaging	<a href="http://www.ti.com/video">www.ti.com/video</a>

### TI E2E Community

[e2e.ti.com](http://e2e.ti.com)